

if  $z$  is not too large. If the reptation time for  $L$  chains is small enough, the contributions of the slowest renewal modes, where the relaxation times are widely spaced, will be negligible. The criterion for validity of the continuous representation is therefore

$$(\tau_d)_L \ll N_L^2(\tau_d)_S \quad (\text{A-2})$$

If  $(\tau_d)_L$  is independent of mixture composition, then  $(\tau_d)_L/(\tau_d)_S = N_L^3/N_S^3$ , and the criterion becomes

$$N_S^3 \gg N_L \quad (\text{A-3})$$

as reported in the text. This is precisely equivalent to  $M_S^3 \gg M_L M_e^2$ , the criterion for case I relaxation behavior in mixtures,<sup>3</sup> i.e., where the relaxation time of  $L$  chains is independent of mixture composition. All mixtures in the present study satisfy that criterion,<sup>3</sup> so the continuous approximation for  $R(t)$  should be quite acceptable here.

**Registry No.** Polybutadiene, 9003-17-2.

## References and Notes

- (1) Current address: Corporate Research Laboratories, Exxon Research and Engineering Co., Annandale, NJ 08801.

- (2) Current address: Paramins Technology Division, Exxon Chemical Co., Linden, NJ 07036.
- (3) Struglinski, M. J.; Graessley, W. W. *Macromolecules* **1985**, *18*, 2630.
- (4) Graessley, W. W. *Faraday Soc. Symp.* **1983**, *18*, 7.
- (5) Ferry, J. D. *Viscoelastic Properties of Polymers*, 3rd ed.; Wiley: New York, 1980.
- (6) de Gennes, P.-G. *J. Chem. Phys.* **1971**, *55*, 572.
- (7) Doi, M.; Edwards, S. F. *J. Chem. Soc., Faraday Trans. 2* **1978**, *74*, 1789.
- (8) Doi, M.; Edwards, S. F. *J. Chem. Soc., Faraday Trans. 2* **1978**, *74*, 1802.
- (9) Graessley, W. W. *Adv. Polym. Sci.* **1982**, *47*, 67.
- (10) Klein, J. *Macromolecules* **1978**, *11*, 852.
- (11) Orwoll, R. A.; Stockmayer, W. *Adv. Chem. Phys.* **1969**, *15*, 305.
- (12) Green, P. F.; Mills, P. J.; Palmstrom, C. J.; Mayer, J. W.; Kramer, E. J. *Phys. Rev. Lett.* **1984**, *53*, 2145.
- (13) Kan, H.-C.; Ferry, J. D.; Fetters, L. J. *Macromolecules* **1980**, *13*, 1571.
- (14) Montfort, J. P.; Marin, G.; Monge, Ph. *Macromolecules* **1984**, *17*, 1551.
- (15) Doi, M. *J. Polym. Sci., Polym. Lett. Ed.* **1981**, *19*, 265.
- (16) Marrucci, G. *J. Polym. Sci., Polym. Phys. Ed.* **1985**, *23*, 159.
- (17) Viovy, J. L., unpublished manuscript.
- (18) Helfand, E.; Rubenstein, M., unpublished manuscript.
- (19) Struglinski, M. J.; Doctoral Thesis, Chemical Engineering Department, Northwestern University, Evanston, IL, 1984.

## Scaling Relations for Aqueous Polyelectrolyte Salt Solutions. 4. Electric Birefringence Decay as a Function of Molar Mass and Concentration

Sybren S. Wijmenga, Frans van der Touw, and Michel Mandel\*

Department of Physical and Macromolecular Chemistry, Gorlaeus Laboratories, University of Leiden, 2300 RA Leiden, The Netherlands. Received October 9, 1985

**ABSTRACT:** The electric birefringence decay of aqueous sodium poly(styrenesulfonate)-0.01 M NaCl solutions with various polyelectrolyte molar mass and concentrations has been studied after the application of rectangular electric field pulses. All decay curves could be represented by a superposition of at least three exponential functions. The longest relaxation time  $\tau_1$  (or the mean relaxation time  $\bar{\tau}$  to which it is proportional) exhibits a different concentration dependence in the dilute and in the semidilute regime. In the former it is nearly concentration independent and may be related to the rotational motion of isolated polyelectrolyte chains, yielding values for the mean-square radius of gyration in good agreement with theoretical predictions based on a wormlike chain approach to polyelectrolytes. In the semidilute regime,  $\tau_1$  and  $\bar{\tau}$  considerably increase with increasing concentration but remain molar mass dependent. The reduced values  $(\bar{\tau}/\tau_d)$ , where  $\tau_d$  refers to the value in the dilute regime, are found to scale like  $(C/C^*)^\beta$  after due correction for the concentration dependence of the ionic strength and to be independent of molar mass,  $C^*$  being the critical concentration and  $\beta = 0.60$ . This can be understood if the renewal time of the chain is expressed by using a "blob" model for the macromolecule, as should apply if the semidilute solutions form transient networks, and is assumed to depend on the numbers of blobs to the power  $\nu = (4\beta + 9)/5 = 2.3$ .

## Introduction

Electric birefringence is observed when a linearly polarized light beam, traveling through an otherwise isotropic system in a direction perpendicular to that of an externally applied field, becomes elliptically polarized due to the induced anisotropy of the refractive index. This Kerr effect is a nonlinear electric field effect and is generally attributed to the orientation of the molecules under the action of the electric field. It thus can be understood in terms of the optical polarizability tensor of the molecules and an orientational function arising from the interaction of the molecules with the electric field. The latter may involve, in a first approximation, permanent dipole moments as well as induced dipole moments. As long as a constant field maintains the polarization of the system, the electric birefringence will tend to a stationary value. Both this stationary value of the birefringence and its time

dependence are determined by the orientational mechanism responsible for the induced anisotropy. Only in the case of solutions of simple molecules and in the approximation of negligible intermolecular interactions has it been possible to derive mathematical expressions for the time dependence and the stationary value of the birefringence after switching on the electric field.<sup>1</sup> For more complicated molecules and, in particular, for macromolecules with a large number of internal degrees of freedom, the situation is much more complicated unless simplifying models are used.<sup>2</sup> In the case of solutions containing charged macromolecules the situation is even more complex because nonconventional polarization phenomena involving perturbation of the small ion distribution by the electric field have probably to be taken into account.

In general the situation is easier to analyze for the opposite case where the electric birefringence spontaneously

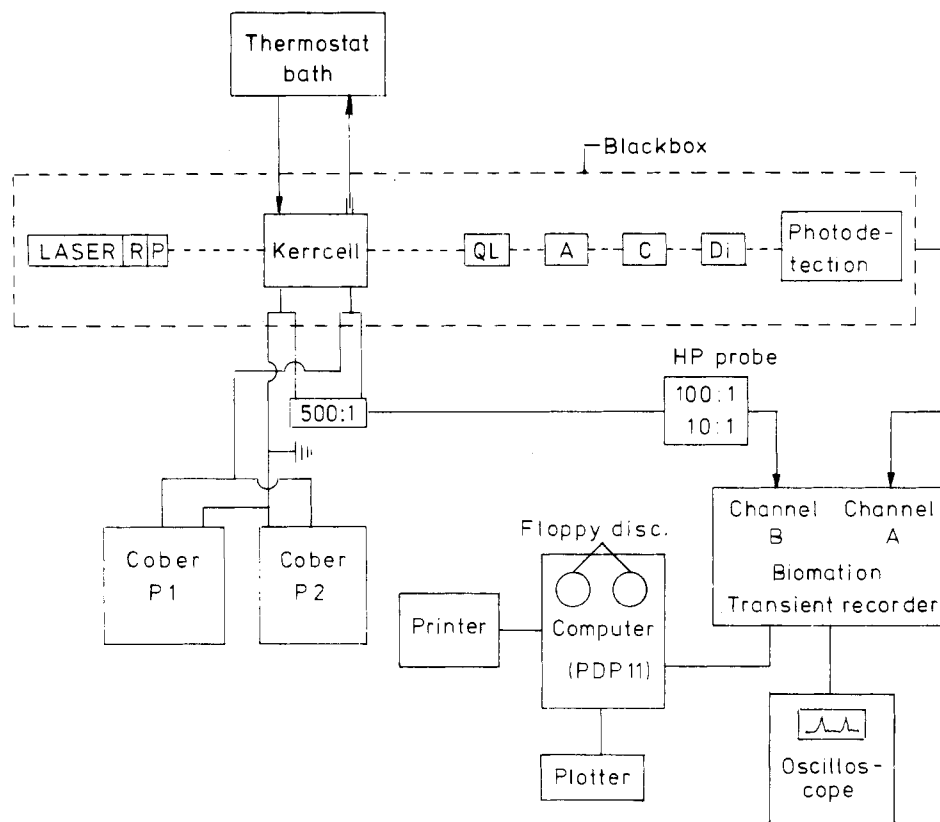


**Figure 1.** Schematic diagram of the birefringence apparatus: (R) rotator; (P) polarizer; (QL) quarter-wave device; (A) analyzer; (C) light chopper; (Di) diaphragm.

disappears on switching off the applied electric field. Here, whatever order there has been induced, it has to disappear through the motion of the solute (and solvent) molecules tending to the equilibrium state in the absence of the field. For simple molecules this will involve rotational diffusion; for more complicated molecules such as macromolecules, both overall rotational diffusion and intramolecular motions of different time and length scales are involved.

We wish to present here an experimental study of the electric birefringence decay after the application of rectangular field pulses to aqueous solutions of sodium poly(styrenesulfonate) (NaPSS) containing 0.01 M NaCl. It represents a systematic investigation of the concentration and molar mass dependence of the decay curves both in the dilute and in the semidilute regime. As will be shown, interesting information concerning the dynamical behavior of charged macromolecules in aqueous salt solutions can be obtained. The electric birefringence decay results seem to confirm previous findings about the distinction between a dilute and a semidilute concentration regime<sup>3</sup> in agreement with theoretical predictions for polyelectrolyte-salt solutions.<sup>4</sup> A preliminary report on the present results has already appeared.<sup>5</sup>

## Experimental Section

**(a) Material.** The sodium salts of poly(styrenesulfonic acid) were of commercial origin (Pressure Chemical Co., Pittsburgh, PA). The different samples, of molar mass  $1.8 \times 10^5$ ,  $4.0 \times 10^5$ ,  $5.9 \times 10^5$ ,  $6.5 \times 10^5$ , and  $10.3 \times 10^5$  g mol<sup>-1</sup>, had been prepared by sulfonation of well-defined, nearly homodisperse samples of polystyrene. According to the manufacturer, the polyelectrolyte samples are characterized by a ratio  $M_w/M_n < 1.1$ . The material purchased was always exhaustively dialyzed against pure water and then freeze-dried.

All solutions were prepared with deionized water and NaCl of analytical grade (Merck). The salt concentration was kept fixed at 0.01 M. Concentrations of NaPSS were determined spectrophotometrically at 261 nm, after calibration with Beer's law taking

into account correction for the water content of the sample (determined by IR absorption of the freeze-dried material dissolved in pure D<sub>2</sub>O).

**(b) Apparatus.** The birefringence apparatus (Figure 1) is fairly standard.<sup>6</sup> The light source is a 5-mW He-Ne laser (Spectra Physics) operating at 632.8 nm. Before it enters the Kerr cell (see hereafter), the laser beam passes through a rotator and a high-quality polarizer (Glan Thompson with extinction ratio  $< 10^{-6}$ ; B. Halle), both mounted on the laser head. The emerging beam goes through a  $\lambda/4$  device (B. Halle) and an analyzer (of the same specifications as the polarizer), both of which can be rotated and their orientation position determined with an accuracy of 0.01° passes through a light-chopper and diaphragm, and finally falls on a photodiode. This photodiode and the coupled amplifier form a fast response detection system. In the least sensitive mode, the output is 4 mV for an input of 5  $\mu$ W of light power with a response time less than 0.5  $\mu$ s. In the most sensitive mode, the output is 1 V for the same input, but the response time is 1.8  $\mu$ s.

The laser, Kerr cell,  $\lambda/4$  plate, and analyzer are each mounted in such a way that their position can be adjusted in three mutually perpendicular directions. The complete optical system is enclosed in a light-tight blackened box positioned on a vibrationally damped table consisting of a table leaf mounted on airlegs (Newport Research Corp.).

The output of the photodetection system is fed into channel A of a Biomation (8100) transient recorder with an 8-bit resolution and a minimal sample time of 0.01  $\mu$ s. Simultaneously, the voltage applied to the electrodes of the Kerr cell is fed into channel B after passing a 500:1 step-down probe and a Hewlett-Packard impedance matching probe operating at an attenuation of 100:1 or 10:1 ratio. Each birefringence curve and attenuated voltage pulse are stored in the 2048 words of digitizer memory and transferred to an on-line PDP 11 computer in the time interval between successive voltage pulses. The computer stores the signals on disks. The birefringence curve and the attenuated voltage are also displayed for control on a CRT screen connected to the transient recorder.

The high voltage pulses are generated by a pulse generator and amplifier (Cober Electronics P202) which can produce voltages between 0 and 2500 V. As the Cober pulse generator works most favorably at an output resistance of 200  $\Omega$ , a high-power switching

board of low inductance is used for impedance matching with the Kerr cell. It is constructed in such a way that it also can act as a voltage divider, applying relatively low voltages to the Kerr cell while the pulse generator operates at a high voltage. The voltage applied was measured directly at the electrodes of the cell by means of a 500:1 step-down probe linked in series to a Hewlett-Packard impedance matching probe operating with an attenuation factor 10:1.

The Kerr cell was of a special construction with a very low intrinsic optical retardation and has been described elsewhere.<sup>7</sup> The optical path length was 70.0 mm and the spacing between the electrodes 1.77 mm. The temperature of the cell was kept constant by circulating water from a thermostat bath (at 21.00 ± 0.05 °C) through a thermostating jacket surrounding the complete cell. Before, during, and after the application of the pulse, the conductivity of the solution in the Kerr cell may be measured by a conductometer Metrohm (E 518).

The direction of polarization of the incident beam makes an angle of 45° with the direction of the applied field, whereas the analyzer is rotated through an angle  $\alpha$  with respect to its position of maximal extinction for the incident beam. The retardation  $\delta$  of the solution can be determined from the change of the intensity of the light falling on the detector after application of the electric field.

$$\frac{\Delta I_d}{I_{\alpha,0}} = \frac{I_{\alpha,0} - I_{\alpha,\delta}}{I_{\alpha,0}} = \frac{\sin^2 \left( \alpha + \frac{\delta}{2} \right) - \sin^2 \alpha}{\sin^2 \alpha} \quad (1)$$

Here  $I_{\alpha,\delta}$  and  $I_{\alpha,0}$  stand for the measured intensity with the field on and the field off respectively. The retardation of the solution, eventually after correction for the intrinsic retardation of the empty cell, is related to the electric birefringence  $\Delta n$

$$\delta(t) = (2\pi/\lambda)l\Delta n(t) \quad (2)$$

where  $\Delta n \equiv (n_{\parallel} - n_{\perp})$  is the difference between the refractive index in a direction parallel to the electric field ( $n_{\parallel}$ ) and the refractive index in the direction perpendicular to it ( $n_{\perp}$ ),  $\lambda$  the wavelength of the light beam in vacuo, and  $l$  the path length of the cell.

The performance of the birefringence system was checked with pure water. A Kerr constant of  $(1.78 \pm 0.03) \times 10^{-20} \text{ m}^2 \text{ V}^{-2}$  was measured, in good agreement with literature values.<sup>6</sup>

**(c) Data Analysis.** The experimentally obtained decay curves were usually fitted to an exponential or a superposition of exponentials by using Marquardt's algorithm<sup>8</sup> incorporated into a Fortran IV program that performs a least-squares fit to a nonlinear equation. The advantage of Marquardt's algorithm over other is that it combines the gradient-search method with the linearization of the fitting function. The gradient search is ideally suited for approaching the minimum from far away, but it does not converge rapidly in its neighborhood. There, the more rapidly converging linearization method can be used. This has the additional advantage not to require very good guesses for the initial parameters.

Because a single decay curve consists of 500–700 points, a fit using all the information would be very time consuming. Therefore the birefringence decay curve normalized to the stationary value was reduced by an appropriate procedure (see Appendix) to a curve of 100 points only. The procedure is such that near  $t = 0$ , where the decay curve is steepest, no averaging is performed, while toward relatively large  $t$  an increasing number of points is being averaged. This ensures that the time constants of the decay curves are not systematically influenced by the reduction procedure.

Quite generally a decay curve is assumed to be represented by a superposition of exponentials. This means for the normalized decay curve that the following expression should hold.

$$\Delta n_n = \left\{ \sum_{k=1}^r A_k \exp(-t/\tau_k) \right\} + A_w \exp(-t/\tau_w) \quad r \geq 1 \quad (3a)$$

$$\sum_{k=1}^r A_k + A_w = 1 \quad (3b)$$

Here the contribution of the solvent has already been separated from the (multi)exponential contribution of the solute. For aqueous solutions the relaxation time  $\tau_w \approx 1 \text{ ns}$  and in general

$\tau_w < \tau_k$ . The relative contribution  $A_w$  can be calculated from the known Kerr constant of water  $K_w$ , viz.  $A_w = K_w E^2 / \Delta n$  ( $t = 0$ ).

Two corrections have to be taken into account. If the response time of the photodetection system  $\tau_D$ , which depends on the amplification ratio, is of the same order of magnitude as the relaxation times  $\tau_k$ , the correct expression for the birefringence decay will be affected by this time constant.<sup>9</sup>

$$\Delta n_n(t) = \sum_{j=1}^{r+1} A_j \{ (\tau_j/\tau_j - \tau_D) \exp(-t/\tau_j) - (\tau_D/\tau_j - \tau_D) \exp(-t/\tau_D) \} \quad (4)$$

Here in the summation over  $j$ , the contribution of the solvent is included. The last expression may be transformed into

$$\Delta n_n(t) = \left\{ \sum_{j=1}^{r+1} A_j' \exp(-t/\tau_j) \right\} - \left\{ \sum_{j=1}^{r+1} A_j (\tau_D/\tau_j - \tau_D) \right\} \exp(-t/\tau_D) \quad (5)$$

which shows that not only an additional exponential with relaxation time  $\tau_D$  will appear but that the relative contributions of the exponentials with relaxation times  $\tau_j$  are also modified if  $\tau_D$  is not negligible compared to  $\tau_j$ .

$$A_j' = (\tau_j/\tau_j - \tau_D) A_j \quad (6)$$

In practice,  $A_j'$  differed from  $A_j$  only for the solutions containing the lowest molar mass of NaPSS investigated.

Another parasitic effect is the base-line drift, which, in principle, can be time-dependent. It turned out that it can be corrected for in a first approximation by using a constant but fittable base-line value.

The normalized decay curves, eventually corrected for the contribution of water and the photodetection time (only necessary for  $M = 1.8 \times 10^5 \text{ g mol}^{-1}$  at the lowest concentration), were fitted to the following function with a maximum of seven adjustable parameters.

$$\Delta n_n^f(t) = \sum_{k=1}^r a_k' \exp(-t/\tau_k) + a_B' \quad r \leq 3 \quad (7)$$

where  $a_k'$  and  $\tau_k$  stand for the least-squares fitted relative contribution and relaxation time  $k$ , respectively, and  $a_B'$  is the fitted value for a floating base line. Three criteria were used to decide whether or not a fit (with the lowest number of adjustable parameters) was satisfactory:

(a) absence of any systematic distribution of the residuals  $R(t_i)$

$$R(t_i) = \Delta n_n(t_i) - \Delta n_n^f(t_i) \quad (8)$$

around zero, as seen from a visual inspection;

(b) the value of the  $Q$ -index, defined for a curve of  $\rho$  points by

$$Q = 1 - \frac{\sum_{i=1}^{\rho} R(t_i)R(t_{i+1})}{\{R(t_i)\}^2} \quad (9)$$

had to be larger than 0.6 to satisfy the condition that the residuals are not correlated;

(c) the variance  $\chi_m^2$ , defined for a fit with  $m$  parameters  $a_i$  to a curve of  $\rho$  points by

$$\chi_m^2 = \frac{1}{\rho - m - 1} \sum_{i=1}^{\rho} \{R(t_i)\}^2 \quad (10)$$

should have decreased significantly on increasing the number  $m$ . A decrease is considered "significant" if the ratio  $\chi_{m'}/\chi_m$  ( $m' < m$ ) is larger than 1.48, corresponding to a probability of 95% that the decrease is not due to random noise.<sup>8</sup>

It was found that for all systems investigated the best fit was obtained with  $r = 3$ . In a few cases where a fit with  $r = 4$  was attempted, the decrease of  $\chi^2$  was not found to be significant. This does not imply that there are no more than three exponentials contributing to the decay curve but rather that the systematic deviations between fitted and experimental decay curves are falling inside the random noise superposed on the experimental curves, this noise ranging from 5% by very low field strengths to 0.2% for higher field strengths.

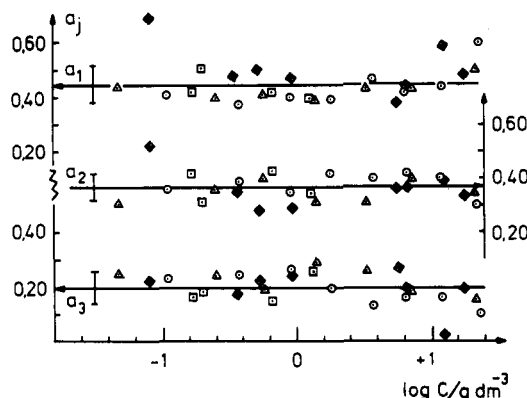


**Figure 2.** Concentration dependence of the coefficients  $a_j$  in the three-exponentials fit to the decay curves for different molar masses:  $1.8 \times 10^5 \text{ g mol}^{-1}$  ( $\diamond$ );  $4 \times 10^5 \text{ g mol}^{-1}$  ( $\square$ );  $5.9 \times 10^5 \text{ g mol}^{-1}$  ( $\triangle$ );  $10.3 \times 10^5 \text{ g mol}^{-1}$  ( $\circ$ ).

For all decay curves the mean relaxation time  $\bar{\tau}$  was obtained by integrating the area under the decay curve. Assuming (4) to be valid, one obtains

$$\int_0^\infty \Delta n_n(t) dt = \left\{ \left( \sum_j A_j \bar{\tau}_j \right) + \bar{\tau}_D \right\} = (1 - A_w) \bar{\tau} + A_w \bar{\tau}_w + \bar{\tau}_D \approx (1 - A_w) \bar{\tau} + \bar{\tau}_D \quad (11)$$

Here the normalization condition for the relative contributions  $A_j$  has been taken into account as well as the condition  $\bar{\tau}_w \ll \bar{\tau}$ . The mean relaxation time is defined by (see eq 3)

$$\bar{\tau} = \sum_k A_k \bar{\tau}_k \quad (12)$$

It follows from (11) that the mean relaxation time may be found from the area under the decay curve by subtracting  $\bar{\tau}_D$  from the integral and dividing the result by  $(1 - A_w)$ .

The integration was performed by using Simpson's method and the complete measured decay curve consisting of 500–700 points each. The inaccuracy of the area was less than 1%.

## Results

Decay curves have been obtained by using field strengths that ranged from 0.3 to 2.6  $\text{kV cm}^{-1}$  for the lower concentrations,  $C < 1.0 \text{ g dm}^{-3}$ . At higher concentrations the maximum value for  $E$  had to be reduced in order to avoid heating of the solution due to the higher conductance. For  $C > 10.0 \text{ g dm}^{-3}$ ,  $E$  had to be limited to 0.3 and even down to 0.1  $\text{kV cm}^{-1}$ . It was found that the values of the three relaxation times  $\tau_1$ ,  $\tau_2$ , and  $\tau_3$  did not depend significantly on the field strength within the range explored. The relative contributions  $a_j'$  somewhat increased with  $E$  for  $E > 1 \text{ kV cm}^{-1}$  for the highest molar masses. The results given for  $\tau_j$  are therefore averages over the complete range of  $E$  values measured, whereas the  $a_j'$  values are the averages for  $E < 1 \text{ kV cm}^{-1}$ . The latter were renormalized to correct for the influence of the base-line  $a_B'$ .

$$a_j = a_j' / (1 - a_B') \quad (13)$$

This renormalization hardly affected the value of these parameters, as in general  $a_B' < 0.015$ .

The values for  $a_j$  for different molar masses and polyelectrolyte concentration have been represented in Figure 2. As can be seen, for each relative contribution  $a_j$  there is no systematic dependence either on  $C$  or on  $M$ . The following mean values can be used for all systems:  $a_1 = 0.45 \pm 0.07$ ;  $a_2 = 0.37 \pm 0.05$ ;  $a_3 = 0.20 \pm 0.06$ , the range of uncertainty representing the standard deviation of all values with respect to the mean. On the contrary, the values of the different relaxation times in general differ from system to system. As an example, the concentration

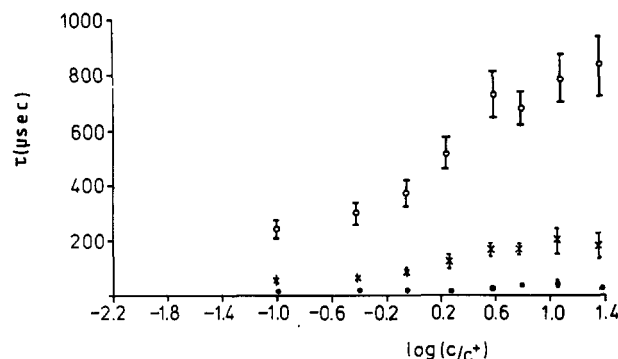


**Figure 3.** Concentration dependence of the three relaxation times  $\tau_1$  ( $\circ$ ),  $\tau_2$  ( $\times$ ), and  $\tau_3$  ( $\bullet$ ) obtained from a three-exponentials fit to the decay curves for  $M = 10.3 \times 10^5 \text{ g mol}^{-1}$  (concentrations reduced to  $C^*$ , calculated according to the theoretical expressions (28) and (29)).

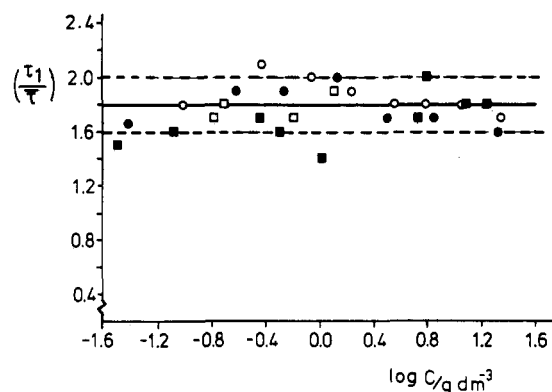


**Figure 4.** Concentration dependence of  $\tau_1/\bar{\tau}$  for four different molar masses investigated:  $1.8 \times 10^5 \text{ g mol}^{-1}$  ( $\blacksquare$ );  $4.0 \times 10^5 \text{ g mol}^{-1}$  ( $\square$ );  $5.9 \times 10^5 \text{ g mol}^{-1}$  ( $\bullet$ );  $10.3 \times 10^5 \text{ g mol}^{-1}$  ( $\circ$ ).

dependence of the three relaxation times obtained for the different solutions with NaPSS of  $M = 1.03 \times 10^6 \text{ g mol}^{-1}$  is shown in Figure 3.

The three-exponentials fit has not been applied to the decay curves of all systems investigated, as it is rather time-consuming. It is much easier to determine from each decay curve the mean relaxation time  $\bar{\tau}$ . In Figure 4 the ratio  $\tau_1/\bar{\tau}$  for 28 different systems has been represented. As may be observed, there is no systematic influence of molar mass or polyelectrolyte concentration on this ratio, the points being distributed around the mean value  $1.8 \pm 0.2$ . This ratio may therefore be considered to be constant within 10%, irrespective of the system investigated.

In order to emphasize the concentration dependence of  $\tau_1$ , the ratio  $\tau_1/(\tau_1)_d$  has been plotted as a function of the logarithm of the reduced concentration ( $C/C^*$ ) in Figure 5. Here  $(\tau_1)_d$  represents the (mean) value of the relaxation time at the lowest concentrations ( $C < 0.5C^*$ ) and  $C^*$  the critical concentration separating the dilute from the semidilute regime according to recent scaling concepts for polymer solutions.<sup>10</sup> These have been shown to apply as well to solutions of polyelectrolytes in the presence of additional salt.<sup>4</sup> (For more details see hereafter.) Figure 5 clearly shows that there is a region below  $C^*$  where  $\tau_1$  is hardly concentration dependent, whereas for  $C/C^* > 1$   $\tau_1$  considerably increases with increasing concentration (values of  $C^*$  were always calculated according to the theoretical expressions).<sup>4</sup> This demonstrates that as far as the first relaxation time is concerned, the distinction between dilute and semidilute regimes very clearly appears. The same is true for  $\bar{\tau}$ . It is also striking that no molar mass dependence in the semidilute regime appears if the results are plotted as in Figure 4, whereas the

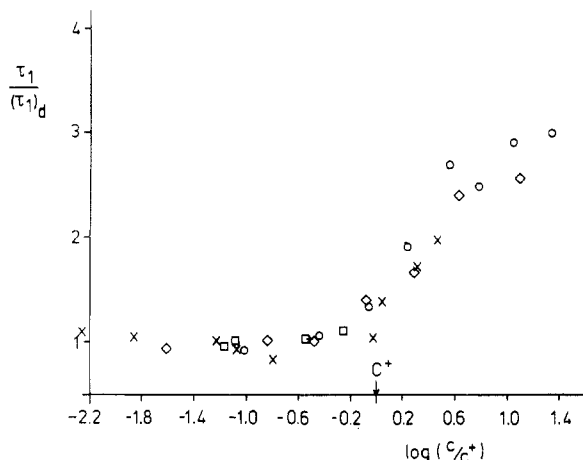


**Figure 5.** Plot of  $\tau_1/(\tau_1)_a$  against the logarithm of the reduced concentration ( $C/C^*$ ) for four different molar masses investigated:  $1.8 \times 10^5 \text{ g mol}^{-1}$  (x);  $4.0 \times 10^5 \text{ g mol}^{-1}$  (□);  $5.9 \times 10^5 \text{ g mol}^{-1}$  (◇);  $10.3 \times 10^5 \text{ g mol}^{-1}$  (○).

"raw" results definitely show a molar mass dependence of  $\tau_1$  or  $\bar{\tau}$  in both the dilute and the semidilute regime.<sup>5</sup>

### Discussion

For a satisfactory description of the electric birefringence decay curves of NaPSS solutions in 0.01 M NaCl, a superposition of at least three exponentials is necessary under all circumstances. Given the quality of the polyelectrolyte samples used, it is unlikely that the distribution of relaxation times can be attributed to a distribution of molar masses. As it has been found from quasi-electric light scattering by the same systems that the poly(styrene-sulfonate) chains in 0.01 M NaCl behave as rather flexible polymers,<sup>3,11,12</sup> the distribution of relaxation times may rather be attributed to the flexibility of the polyelectrolyte chain. The dynamics of such a chain are to be decomposed into contributions of a series of different modes, as already described by Rouse<sup>13</sup> using a spring and bead model. This approach has been extended by Zimm,<sup>14</sup> who introduced hydrodynamic interactions into the model. It has been shown that these modes will show up as different exponentials in the electric birefringence decay curves of chains which have a permanent dipole component parallel to the chain contour.<sup>2</sup> According to Stockmayer,<sup>15</sup> the first mode describing the nontranslational motion of the flexible chain is the overall rotation of the macromolecules and determined by the radius of gyration in the case of dilute solutions.

In the case of polyelectrolyte solutions the mechanism responsible for the birefringence is probably more complicated than in the case of unchanged macromolecules. It may, however, also be assumed that the decay of the birefringence is related to the motions of the chain after the orientational constraints imposed by the electric field have disappeared. A prerequisite condition is that at least one of the dipole moments involved in the establishment of the birefringence should have a component parallel to the end-to-end vector of the macromolecule,<sup>15</sup> a condition which seems to be satisfied. This conclusion follows from an analysis of the stationary Kerr constants observed for the same solutions, which will be published in a subsequent paper.<sup>16</sup> Another condition should be that the lifetime of that dipole moment is longer than the characteristic time necessary for the rotational or intramolecular motion, contributing to the relaxation times observed. Otherwise the decay of the birefringence may be determined by the "rapid" decay of that dipole moment or, at least, considerably influenced by the latter in a complicated way.

Although in the mode analysis according to Zimm the relative contribution of higher modes rapidly decreases, it is not to be expected that in the birefringence decay curve only three modes will show up. The limitation of the fit to a superposition three exponentials only should rather be attributed to the effect of the random noise. In fact, a simulated decay curve consisting of eight exponentials with relative contributions and relaxation times calculated according to the Zimm model could be fitted to a superposition of at least five exponentials provided the random noise superposed on the simulated curve did not exceed a contribution of 0.1%. For larger contributions—corresponding more realistically to the conditions of the experimental equipment used—only a three-exponentials fit proved feasible within the criteria used. Only the first relaxation time and its relative contribution corresponded to the values of the parameters introduced into the simulation, whereas both  $a_j$  and  $\tau_j$  (for  $j = 2$  or  $3$ ) contained contributions of several higher modes.

It is therefore tempting to assume that the first relaxation time, obtained from a three-exponentials fit to the experimental decay curves, is related to the overall motion of the polyelectrolyte chain in our polyelectrolyte systems. This would imply that  $\bar{\tau}$ , proportional to  $\tau_1$ , is also related to that motion. Interpretation of the relaxation times  $\tau_2$  and  $\tau_3$  will not be easy as long as an improved fitting procedure to decay curves remains difficult and will therefore not be attempted. It is also highly probable that in the dilute regime, where intermolecular interactions are weak, the first relaxation time is directly related to the rotational motion of the isolated macromolecule. In the semidilute regime, where transient networks are to be expected through the interpenetration of the polyelectrolyte chains, the overall polyelectrolyte motion may be more complicated. In view of the clear distinction between the dilute and the semidilute concentration regimes that can be observed insofar as the first relaxation times  $\tau_1$  of the electric birefringence decay curves or  $\bar{\tau}$  are concerned, we shall discuss the results in the dilute regime in terms of  $(\tau_1)_a$ , as defined above, and in the semidilute regime in terms of  $\bar{\tau}$ , of which more values are available.

**Dilute Regime.** In the Zimm model,<sup>14</sup> strictly applicable to  $\theta$ -conditions, the longest relaxation time for a flexible chain at infinite dilution is given by

$$(\tau_1)_\theta = (1/p)(\Phi_0 \eta_s 6^{3/2} \langle S^2 \rangle_0^{3/2} / N_A v k T) \quad (14)$$

Here  $\Phi_0 = 2.84 \times 10^{23}$  is the draining parameter,  $\eta_s$  the solvent viscosity,  $\langle S^2 \rangle_0$  the mean-square radius of gyration under  $\theta$ -conditions,  $N_A$  Avogadro's constant,  $k$  the Boltzmann constant,  $T$  the temperature (in Kelvin) and  $p$  a numerical factor ( $p = 2.38$ ). In case excluded-volume effects have to be taken into account, it has been shown<sup>17</sup> that an equation analogous to (14) is valid, using the mean-square radius of gyration under perturbed conditions  $\langle S^2 \rangle$  and  $\Phi_0' = 1.81 \times 10^{23}$ , provided the expansion factor  $\alpha_s$  for the radius of gyration is related to the contour length  $l$  of the macromolecule by the limiting condition  $\alpha_s \sim l^{0.1}$ .

$$\tau_1 = (1/p)(\Phi_0' \eta_s 6^{3/2} \langle S^2 \rangle^{3/2} / N_A v k T) \quad (15)$$

Analogous equations, differing only through numerical factors, are obtained in the Kirkwood-Riseman approach.<sup>18</sup> Here the rotational motion of the chain is expressed with the help of its average dimensions leading to the following rotational diffusion coefficient  $D_r$ .

$$D_r = N_A v k T / (4M \eta_s [\eta]) \quad (16)$$

Here  $M$  and  $[\eta]$  stand for the molar mass and the intrinsic viscosity, respectively, of the macromolecule. Under  $\theta$ -

conditions and for the nondraining case the latter is given by

$$[\eta]_0 = \Phi_0'' 6^{3/2} \langle S^2 \rangle_0^{3/2} / M \quad (17)$$

with the draining parameter  $\Phi_0'' = 2.87 \times 10^{23}$ . As for a rigid particle, the Kerr relaxation time  $\tau_1$  is related to  $D_r$  by<sup>19</sup>

$$\tau_1 = \frac{1}{6} D_r \quad (18)$$

Substitution of (16) and (17) into (18) yields the following expression, to be compared to (14).

$$(\tau_1)_0 = (1/p) (\Phi_0'' \eta_s 6^{3/2} \langle S^2 \rangle_0^{3/2} / N_A \nu kT) \quad (19)$$

Here  $p = 1/6 = 1.5$ . Under perturbed conditions and provided the excluded-volume effect is isotropic, (16) remains valid with  $[\eta]_0$  replaced by  $[\eta]$

$$[\eta] = [\eta]_0 \alpha_\eta^3 \quad (20)$$

where  $\alpha_\eta$  is the viscosity expansion factor. Combining (16)–(18) and (20), we obtain for the relaxation time under perturbed conditions

$$\tau_1 = (1/p) (\Phi_0'' \eta_s 6^{3/2} \langle S^2 \rangle_0^{3/2} / N_A \nu kT) \quad (21)$$

with  $\Phi = \Phi_0'' (\alpha_\eta / \alpha_s)^3$ . It is generally admitted that  $\alpha_\eta$  and  $\alpha_s$ , although related, should differ.<sup>17</sup>

$$\alpha_\eta^3 = \alpha_s^2 \alpha_D \quad (22)$$

$\alpha_D$  represents the expansion factor of the reciprocal average end-to-end distance. According to Weill and des Cloizeaux<sup>20</sup> the ratio  $\Phi / \Phi_0'' = \alpha_D / \alpha_s$  reaches a limiting value 0.78 for large values of  $\alpha_s$ .

In both cases  $\tau_1$  in the dilute regime should be proportional to  $\langle S^2 \rangle_0^{3/2} \eta_s / kT$  for flexible chains. Thus  $\tau_1$  can be used for the comparison of the root mean square radius of gyration of different macromolecules in the same solvent and constant temperature, provided they satisfy the condition of having flexible chains.

For polyelectrolytes in the presence of an excess salt, the wormlike chain approach as developed by Odijk<sup>21</sup> and Fixman and Skolnick<sup>22</sup> allows a theoretical estimate for  $\langle S^2 \rangle$ .

$$\langle S^2 \rangle = \alpha_s^2 (Z_{el}) \langle S^2 \rangle_0 \quad (23a)$$

$$\langle S^2 \rangle_0 = 2lL_t \{ 6^{-1} - 2^{-1}(L_t/l) + (L_t/l)^2 - (L_t/l)^3 [1 - \exp(-l/L_t)] \} \quad (23b)$$

Here  $\alpha_s (Z_{el})$  represents the expansion factor depending on the excluded-volume parameter  $Z_{el}$  assumed to be determined by screened electrostatic interactions only between Kuhn's segments of length  $2L_t$ , with  $L_t$  the persistence length. The expression of the unperturbed mean square radius of gyration (23b) has been derived by Benoit and Doty<sup>23</sup> for a wormlike chain of persistence length  $L_t$  and contour length  $l$ . For polyelectrolytes the total persistence length can be split up into an intrinsic part  $L_p$  and an electrostatic part  $L_e$  due to short-range charge interactions along the chain. According to the theory

$$L_t = L_p + L_e = L_p + (Q/4\kappa^2 A^2) f^2 \quad (24)$$

where  $Q = q^2/4\pi\epsilon_0 kT$  represents the Bjerrum length ( $q$  being the elementary charge,  $\epsilon_0$  the permittivity of free space, and  $\epsilon$  the relative permittivity of the solvent),  $\kappa^{-1}$  the Debye screening length defined through  $\kappa^2 = 8\pi QI$  with  $I$  the ionic strength of the solution,  $A$  the contour distance between two successive charges on the chain (for a po-

Table I

$M \times 10^{-5}$ , g mol <sup>-1</sup>	$(\tau_1)_d$ , $\mu$ s	$\langle S^2 \rangle_{exp}^{1/2}$ , nm	$\langle S^2 \rangle_{th}^{1/2}$ , nm	$R_F$ , nm	$C^*$ , g dm <sup>-3</sup>
1.8	6.6 ± 0.9	25 ± 1	28	43	3.9
4.0	37 ± 4	44 ± 2	45	69	2.0
5.9	92 ± 4	59 ± 1	58	87	1.5
6.5	118 ± 15 <sup>c</sup>	64 ± 3	61	92	1.4
10.3	245 ± 30	82 ± 3	79	121	1.0

<sup>a</sup>  $\langle S^2 \rangle_{exp}$  derived from (15). <sup>b</sup>  $\langle S^2 \rangle_{th}$  derived from (23), (24), (26), and (27). <sup>c</sup> Determined at only one concentration,  $C = 0.54$  g cm<sup>-3</sup>.

lyelectrolyte carrying one elementary charge per monomeric unit also equal to the length  $a$  of a monomeric unit), and, finally,  $f$  a factor which eventually takes into account that strong interactions between the charged chain and the counterions in solution may reduce the effective charge of the polyion,  $0 < f < 1$ . As a lower limit for  $f$  the value  $f = \lambda^{-1} \equiv (A/Q)$ , as predicted by the condensation approach,<sup>24-27</sup> may be used for polyelectrolytes satisfying the condition  $\lambda > 1$ , as is the case for poly(styrenesulfonate) at room temperature in water. The ionic strength of the solution,  $I$ , for the polyelectrolyte solution of equivalent concentration  $c$  in the presence of a mono-monovalent salt of concentration  $c_s$  (both in mol dm<sup>-3</sup>) is given by

$$I = 10^3 N_A [c_s + (cf/2)] \quad (25)$$

taking into account the contribution of the "free" counterions only provided by the polyelectrolyte chains.

A theoretical expression for the excluded-volume parameter has been proposed by Fixman and Skolnick<sup>28</sup> and takes the following form if the factor  $f$  is consistently introduced.

$$Z_{el} = (3^{3/2}/16\pi^{1/2}) \kappa^{-1} \{ \ln(4\pi f/A\kappa) + \gamma - 0.5 \} l^{1/2} L_t^{-3/2} \quad (26)$$

Here  $\gamma = 0.57721 \dots$  is Euler's constant. The expansion factor  $\alpha_s$  is given by perturbation theory as a series expansion in  $Z$ .<sup>17</sup> An approximate closed expression for  $\alpha_s$ , which gives correct values for both small and very large values of  $Z$ , has been proposed by Yamakawa and Tanaka<sup>29</sup> and may be used to estimate the expansion factor in the case of polyelectrolytes in the presence of an excess of salt.<sup>17,30</sup>

$$\alpha_s^2 = 0.541 + 0.549(1 + 6.04Z_{el})^{0.46} \quad (27)$$

With the help of eq 23–27 the mean-square radius of gyration may be estimated. For very dilute solutions the assumption  $f = \lambda^{-1}$  may be used as a good first approximation. Values of  $\langle S^2 \rangle^{1/2}$  calculated from the experimental  $(\tau_1)_d$  data according to (15) are compared to the theoretical values, derived as explained above, in Table I. For the latter the value of  $l$  was estimated by assuming that a monomer has a length  $a = A = 0.25$  nm and that  $L_p = 1$  nm; for the former the limiting value  $\Phi/\Phi_0'' = 0.78$  was used as, according to (27),  $\alpha_s^2 > 4$  for all systems investigated.

The agreement between the values estimated from (15) and the theoretical predictions based on the wormlike chain approach is quite good, in spite of a number of approximations that had to be used. This agreement supports the conclusion that in the dilute regime the longest relaxation time of the electric birefringence decay, as observed with rectangular pulses, is essentially determined by the average mean-square radius of gyration of the polyelectrolyte in a way consistent with the overall rotation of the macromolecule.

**Semidilute Regime.** As indicated above, the separation between dilute and semidilute regimes is assumed to occur

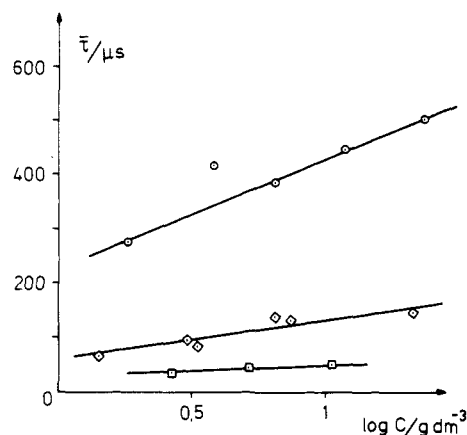


**Figure 6.** Concentration dependence of  $\bar{\tau}$  in the semidilute range for three different molar masses:  $4.0 \times 10^5 \text{ g mol}^{-1}$  ( $\square$ );  $5.9 \times 10^5 \text{ g mol}^{-1}$  ( $\diamond$ );  $10.3 \times 10^5 \text{ g mol}^{-1}$  ( $\circ$ ).

in a concentration region characterized by a critical concentration  $C^*$ , which is defined by the following relation.<sup>10</sup>

$$C^* = (l/a)(M_m/N_{Av})R_F^{-3} \quad (28)$$

Here  $M_m$  is the molar mass of the monomeric unit and  $C^*$  is expressed in g per unit volume. The Flory radius  $R_F$  is, in the scaling approach, to be defined as the root mean square radius of gyration of the polymer in a good solvent under the conditions that  $(l/L_t) \rightarrow \infty$ , i.e., that  $\langle S^2 \rangle_0 \sim lL_t$  and  $\alpha_s \sim Z^{1/5}$ . For polyelectrolytes in the presence of excess salt, the Flory radius can easily be derived from (23) and can be put into the following form<sup>4</sup>

$$R_F \simeq l^{3/5}(L_t/\kappa)^{1/5} \quad (29)$$

where  $\simeq$  means "equal to within a factor of order unity". It follows that  $C^*$  will decrease with increasing molar mass of the polyelectrolyte and decrease with increasing salt concentration. Values of  $R_F$  and  $C^*$  for the different polyelectrolytes used have been evaluated and collected in Table I. As can be seen values of  $R_F$  are 50% larger than the corresponding theoretical values of  $\langle S^2 \rangle^{1/2}$  due to the omission of the numerical factor in (29).

As indicated already above, the electric birefringence decay in the semidilute regime, i.e., for  $C > C^*$ , will be discussed in terms of  $\bar{\tau}$ . This mean relaxation time has been found to increase with increasing polyelectrolyte concentration in the semidilute regime, this increase being steeper the larger the molar mass (Figure 6). As was already mentioned in the preceding section, no molar mass dependence is observed if the reduced relaxation time  $\tau_1/(\tau_1)_d$  or  $\bar{\tau}/\tau_d$  is plotted against the reduced concentration  $C/C^*$ . The molar mass dependence of  $\bar{\tau}$  or  $\tau_1$  itself is in sharp contrast to what is observed in the semidilute regime of the same system with quasi-electric light scattering.<sup>3</sup> There the mean relaxation time of the light intensity correlation function is found to be molar mass independent, in agreement with theoretical predictions<sup>10</sup> that is should be determined by the average molar mass independent correlation length  $\xi$  of the dynamic network arising through chain entanglements. This difference should be related to the fact that in electric birefringence decay measurements rather more complicated chain motions determine the effects observed. The relaxation of the chain from its conformational state, as determined by the presence of an electric field, to new equilibrium conditions when the latter disappears is possibly related to a reptation mechanism. Reptation has been defined as a wormlike motion of a macromolecule moving within constraints arising from other chains, as in a network or a concentrated

solution.<sup>10,31</sup> This situation has been described by Edwards<sup>32</sup> using the model of a chain trapped in a flexible tube formed by its surrounding and being continuously modified during the process of the chain. In this reptation model a characteristic quantity is the reptation time  $\tau_R$ , defined as the average time required for a complete renewal of the chain configuration. It is assumed in the model that after one time interval  $\tau_R$  all memory of the original conformation of the chain has been lost. It is therefore a plausible assumption that  $\tau_1$ , and therefore also  $\bar{\tau}$ , is directly related to  $\tau_R$ .

$$\bar{\tau} \sim \tau_1 \simeq \tau_R \quad (30)$$

A scaling relation can be derived for the reptation time in terms of the number of statistical elements  $N$  in the chain and the average number of  $g$  in the "blobs" of size  $\xi$  necessary to describe the average dimensions in the semidilute regime.<sup>10</sup>

$$\tau_R \simeq (N/g)^3 \xi^3 (6\pi\eta_s/kT) \quad C \gg C^* \quad (31)$$

When the expression for  $g$  and  $\xi$  derived for polyelectrolytes in the presence of excess salt<sup>4</sup> is introduced into (31), a relation between  $\bar{\tau}$ , the contour length or molar mass, and the polyelectrolyte concentration can be derived by assuming the validity of (30).

$$\bar{\tau} \sim \tau_1 \sim l^3 (aC)^{3/2} (L_t/\kappa)^{3/2} (\eta_s/kT) \quad (32)$$

In order to check the concentration dependence of  $\bar{\tau}$  according to the theoretical expression (32), it is important to keep in mind that according to (25) the ionic strength of the solution—and therefore also  $(L_t/\kappa)$ —will depend on the macromolecular concentration in the semidilute regime. It is thus preferable to correct for this ionic strength variation by considering the auxiliary quantity  $B_b$  defined as follows:

$$B_b \equiv \bar{\tau} (L_t/\kappa)^{-3/2} \sim l^3 C^{3/2} \quad C \gg C^* \quad (33)$$

According to theoretical predictions  $B_b$  should increase with concentration according to a  $C^{3/2}$  law. This apparently is satisfied by the experimental results, as  $B_b^{1/3}$  has been found<sup>5</sup> to depend linearly on  $C^{1/2}$  if it is assumed again that  $L_p = 1 \text{ nm}$  and  $f = \lambda^{-1}$ . However, the slopes of the lines  $B_b^{1/3}$  vs.  $C^{1/2}$  were found to depend on a power of  $l$  definitely smaller than unity, contrary to the prediction of (33). Therefore, the molar mass dependence of  $\bar{\tau}$  is not in agreement with the prediction of this simple reptation approach.

Possibly the rather small number of "blobs" per chain (in the case of the PSS investigated  $N/g \leq 20$ ) might be responsible for this disagreement. According to Klein<sup>33</sup> tube reorganization in concentrated or semidilute solutions should occur at a much shorter time scale than for reptation in a fixed network, which was considered originally by de Gennes,<sup>31</sup> provided the number of constraints per chain is small. In that case the exponent of  $l$  in the expression for the renewal time would be smaller than 3. In fact, in the extreme case that the chain of blobs, which can be considered as a Rouse chain of blobs, is not confined to a tube but can move freely, as in the dilute regime, the fundamental relaxation time is given by

$$\tau_{Ro} \simeq (N/g)^2 \xi^3 (6\pi\eta_s/kT) \quad (34)$$

Another limitation of the reptation model, leading to (31), is that in the semidilute regime it is assumed that backflow effects or hydrodynamic interactions between "blobs" are completely screened off, i.e., that the hydrodynamic screening length  $K$  is taken equal to  $\xi$ . If, however,  $K > \xi$ , the molar mass dependence of the chain renewal time



may be affected. In the limit, e.g., where  $K$  would be of the order of the mean dimensions of the chain, the friction coefficient in the semidilute regime would be given by  $F \approx 6\pi\eta_s(N/g)^{1/2}\xi$ , the chain being considered as an ideal chain of "blobs". If in the case the macromolecules is not restricted in its movement by surrounding chains, the fundamental relaxation time would be given by

$$\tau_R \approx (N/g)\xi^2(F/kT) = (N/g)^{3/2}\xi^3(6\pi\eta_s/kT) \quad (35)$$

whereas if the chain would be enclosed in an infinitely long tube, to take the other but rather unrealistic extreme, the reptation time would be given by

$$\tau_R \approx (N/g)^2\xi^2(F/kT) = (N/g)^{5/2}\xi^3(6\pi\eta_s/kT) \quad (36)$$

It follows that various models based on the blob model for the chain in the semidilute regime lead to an expression for the chain renewal time of the general form

$$\tau_R \approx (N/g)^\nu \xi^3(6\pi\eta_s/kT) \quad (37)$$

where  $\nu$  is an exponent which may be different from three. Considering that according to the scaling approach

$$\xi \approx R_F(C^*/C)^{3/4} \approx g^{3/5}L_t^{1/5}\kappa^{-1/5} \quad (38)$$

it follows from (37) by using (28) and (29)

$$\tau_R \sim l^\nu(L_t/\kappa)^{3(\nu-1)/4}C^{(5\nu-9)/4} \quad (39)$$

$$\tau_R/(\tau_1)_d \sim (C/C^*)^{(5\nu-9)/4} \quad (40)$$

This last expression is consistent with the experimental finding that  $\tau_1/(\tau_1)_d$  is a unique function of  $(C/C^*)$  and independent of molar mass if it is assumed that  $\tau_1 \approx \tau_R$  in the semidilute regime. The same should hold for  $\bar{\tau}/\bar{\tau}_d$ .

Equation 40 has been derived by assuming that the ionic strength of the solution, and thus also  $L_t/\kappa$ , is constant in the whole concentration range considered. If in the semidilute regime we take into account the influence of the polyelectrolyte concentration on  $I$ , as in (25), (40) may be reformulated in the following way:

$$\tau_R/(\tau_1)_d \sim (C/C^*)^{(5\nu-9)/4}k^{3(1-\nu)/4} \quad (41)$$

$$k \equiv (L_t/\kappa)_0/(L_t/\kappa)_C \quad (42)$$

Here the index  $C$  refers to the value at the actual polyelectrolyte concentration in the semidilute range  $C$  and the index  $0$  to the value for  $C \rightarrow 0$ . In establishing (41) it has been assumed that consistent with the scaling approach,  $R_F$  is determined by a  $C$ -independent ionic strength  $(L_t/\kappa)_0$  but that the correlation time  $\xi$  depends on the actual ionic strength,<sup>3,4</sup> thus satisfying the following expression instead of (38).

$$\xi \approx R_F(C^*/C)^{3/4}k^{1/4} \quad (43)$$

Equation 41 shows that  $\tau_R/(\tau_1)_d k^{3(1-\nu)/4}$ , and not  $\tau_R/(\tau_1)_d$  itself, should scale like  $(C/C^*)^\beta$ , with  $\beta = (5\nu - 9)/4$ . It follows that the check on (41) and the determination of  $\nu$  requires an iteration procedure. In the first step (40) is assumed to be valid, and a first estimate  $\nu'$  is obtained from the linear least-squares slope of  $\log(\bar{\tau}/\bar{\tau}_d)$  as a function of  $\log(C/C^*)$ . In the second step  $\log(\bar{\tau}/\bar{\tau}_d)k^{\gamma'}$  is used with  $\gamma' = 3(1 - \nu')/4$ , and a better estimate  $\nu''$  is obtained. This procedure is repeated until successive values for these estimates do not change anymore. If points for the system with  $M \geq 4 \times 10^5$  g mol<sup>-1</sup> are used, a few steps only are necessary and a very reasonable linear fit is obtained with a value  $\beta = 0.60 \pm 0.04$  or  $\nu = 2.3 \pm 0.2$  (Figure 7). Note that a value of  $\nu = 2.3$  is not unexpected in view of the discussion given above. For the system with the lowest molar mass and  $l = 215$  nm, the validity of the "blob"

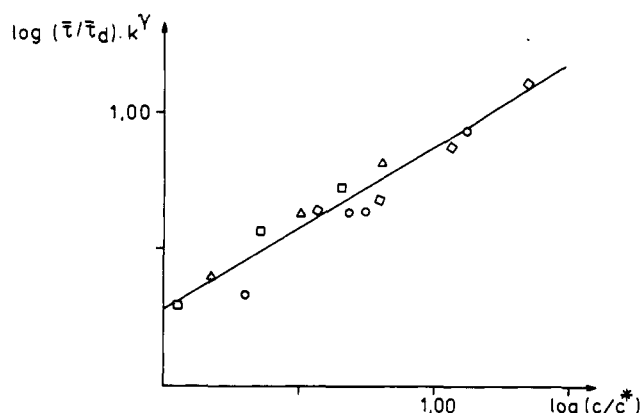


**Figure 7.** Plot of the function  $\log(\bar{\tau}/\bar{\tau}_d)k^\gamma$  vs.  $\log(C/C^*)$  with  $\gamma = 3(\nu - 1)/4$  in the semidilute range (see text); molar masses:  $4 \times 10^5$  g mol<sup>-1</sup> ( $\square$ );  $5.9 \times 10^5$  g mol<sup>-1</sup> ( $\diamond$ );  $6.5 \times 10^5$  g mol<sup>-1</sup> ( $\triangle$ );  $10.3 \times 10^5$  g mol<sup>-1</sup> ( $\circ$ ).

model may be questionable and, anyway, the values of  $(C/C^*)$  are all close to unity.

The conclusion seems justified that in the semidilute regime the value of  $\bar{\tau}$ , and therefore also  $\tau_1$ , is essentially determined by an overall motion of the macromolecule tending to an equilibrium configuration after disappearance of the polarizing electric field. In this regime the chain should be represented by a "blob" model, provided the molar mass is sufficiently high. It is at present and with the information available, however, premature to speculate about the exact mechanism underlying that motion.

## Conclusions

The electric birefringence decay curves observed with NaPSS solutions in aqueous 0.01 M NaCl with various polyelectrolyte molar mass and concentrations, to which rectangular electric field pulses had been applied, are all nonsingle exponentials. The longest relaxation time (or the mean relaxation time to which it is found to be proportional) exhibits a different concentration dependence in the dilute and in the semidilute regime. In the former it is related to the overall rotational motion of an isolated chain; in the latter—where it considerably increases with concentration—it can be understood in terms of the renewal time of a chain consisting of "blobs".

**Acknowledgment.** These investigations have been carried out under the auspices of the Netherlands Foundation for Chemical Research (SON) and with financial aid from the Netherlands Organization for the Advancement of Pure Research (ZWO).

## Appendix

In order to speed up the fitting procedure, a normalized decay curve consisting of 500–700 ( $W$ ) points was replaced by a reduced curve having only 100 points. The time axis was divided into 100 intervals of increasing length, and the original points within each interval were averaged to yield one new point. The original normalized decay curve with  $W$  points equally spaced on the time axis with intervals  $\Delta t$  can be represented by a superposition of  $r$  different exponentials of relative contributions  $a_k$  and relaxation times  $\tau_k$ , with  $\tau_1 > \tau_2 > \dots > \tau_r$ .

$$\Delta n_r(j) = \sum_{k=1}^r a_k \exp(-j\Delta t/\tau_k) \quad 0 \leq j \leq W \quad (\text{A.1})$$

The sample time usually satisfies the condition  $\tau_r > \Delta t \approx 4\tau_1/W$ . The reduced curve  $\Delta n_r^R$  should have the form



$$\Delta n_n^R(s) = \sum_{k=1}^r a_k \exp(-t_s/\tau_k) \quad 0 \leq s \leq 100 \quad (\text{A.2a})$$

$$t_s = \sum_{i=1}^s \Delta t_i \quad (\text{A.2b})$$

$$\sum_{i=1}^{100} \Delta t_i = W\Delta t \quad \Delta t_i \geq \Delta t \quad \Delta t_{i+1} \geq \Delta t_i \quad (\text{A.2c})$$

In order to define the intervals  $\Delta t_i$ , the  $y$ -axis between 0 and 1 is divided into 100 equal intervals  $\Delta y_i = 0.01$ . Each interval has an upper bound  $y_a(i)$  and a lower bound  $y_b(i)$ .

$$y_a(i) = 1 - 0.01(1 - i) \quad y_b(i) = 1 - 0.01i$$

The corresponding points on the time axis, defining the time interval  $\Delta t_i'$ , are derived by approaching the real decay curve by a single exponential of the form  $y \approx \exp(-t/\theta)$ .

$$t_a(i) = -\theta \ln \{1 - 0.01(i - 1)\} \quad t_b(i) = -\theta \ln \{1 - 0.01i\}$$

Consequently the time interval  $\Delta t_i'$  corresponding to  $\Delta y_i$  is given by

$$\Delta t_i' = t_b(i) - t_a(i) = \theta \ln \{1 + (0.01/1 - 0.01i)\} = \theta \ln \phi_i \quad (\text{A.3})$$

The point on the original discontinuous time scale lying within  $\Delta t_i'$  closest to  $t_b(i)$  will be  $j_b(i)$  and analogously there is a point  $j_a(i)$ . We now define the time interval  $\Delta t_i$  in the following way:

$$\begin{aligned} \Delta t_i &= t_b(i) - t_a(i) + \Delta t = \{j_b(i) - j_a(i) + 1\} \Delta t \\ &= \Delta t_i' + \Delta t = \theta \ln \phi_i + \Delta t \end{aligned} \quad (\text{A.4})$$

For the real multiexponential decay curve, the average value of  $\Delta n_n$  in an interval  $\Delta t_i$ , i.e.,  $\Delta n_n^R(i)$ , is given by

$$\begin{aligned} \Delta n_n^R(i) &= \frac{\Delta t}{\Delta t_i'} \sum_{j=j_a(i)}^{j_b(i)} \left[ \sum_{k=1}^r a_k \exp(-j\Delta t/\tau_k) \right] \\ &= \frac{\Delta t}{\Delta t_i'} \sum_{k=1}^r a_k \left[ \sum_{j_a(i)}^{j_b(i)} e^{-j\Delta t/\tau_k} \right] \\ &= \sum_{k=1}^r a_k \frac{\sinh(\Delta t_i/2\tau_k)}{(\Delta t_i/2\tau_k)} \frac{(\Delta t/2\tau_k)}{\sinh(\Delta t/2\tau_k)} \exp\left\{-\left[t_a(i) + \frac{t_b(i)}{2}\right]/2\tau_k\right\} \end{aligned} \quad (\text{A.5})$$

where (A.2–A.4) have been used. The last expression may be rewritten as

$$\Delta n_n^R(s) = \sum_{k=1}^r \tilde{a}_k \exp(-t_s/\tau_k) \quad (\text{A.6a})$$

$$\tilde{t}_s = [t_a(s) + t_b(s)]/2 \quad (\text{A.6b})$$

$$\tilde{a}_k(s) = a_k \left[ \frac{\sinh(\Delta t_s/2\tau_k)}{(\Delta t_s/2\tau_k)} \frac{(\Delta t/2\tau_k)}{\sinh(\Delta t/2\tau_k)} \right] = a_k B_k(s) \quad (\text{A.6c})$$

The value of  $\theta$  (which determines through (A.4) the length

of the time intervals  $\Delta t_i$ ) must be chosen in such a way that no information is lost and that no significant distortion of the decay curve occurs, i.e., that all  $B_k$  values are close to unity in the relevant time interval  $0 < t_s < 4\tau_k$  where the exponential significantly differs from 0. A normal and satisfying choice turns out to be  $\theta \approx \tau_1$ , which not only ensures the already mentioned condition for  $B_k$  but also for the first 10 intervals  $\Delta t_i \approx \Delta t$ . Hence for small  $t$  no averaging is performed and no information is lost concerning the smallest time constants.

## References and Notes

- (a) Buckingham, A. D. In *Molecular Electro-Optics*; O'Konski, C. T., Ed.; Dekker: New York, 1976; Part I, Chapter 2. (b) O'Konski, C. T.; Krause, S. In *Molecular Electro-Optics*; O'Konski, C. T., Ed.; Dekker: New York, 1976; Part I, Chapter 3.
- Jernigan, R. L.; Thompson, D. S. In *Molecular Electro-Optics*; O'Konski, C. T., Ed.; Dekker: New York, 1976; Part I, Chapter 5.
- Koene, R. S.; Mandel, M. *Macromolecules* **1983**, *16*, 220.
- Odijk, T. *Macromolecules* **1979**, *12*, 688.
- Wijmenga, S. S.; van der Touw, F.; Mandel, M. In *Physical Optics of Dynamic Phenomena and Processes in Macromolecular Systems*; Sedlacek, B., Ed.; de Gruyter: Berlin, New York, 1985; p 87.
- Fredericq, E.; Houssier, C. *Electro Dichroism and Electric Birefringence*; Clarendon: Oxford, 1973.
- Wijmenga, S. S.; van der Touw, F.; Mandel, M. *J. Phys. E* **1985**, *18*, 673.
- Bevington, P. R. *Data Reduction and Error Analysis for Physical Sciences*; McGraw Hill: New York, 1969.
- Dieckmann, S.; Hillen, W.; Morgeneyer, B.; Wells, R. D.; Pörschke, D. *Biophys. Chem.* **1982**, *15*, 263.
- de Gennes, P. G. *Scaling Concepts in Polymer Physics*; Cornell University: Ithaca, NY, 1979.
- Koene, R. S.; Nicolai, T.; Mandel, M. *Macromolecules* **1983**, *16*, 227, 231.
- Odijk, T. In *Ionic Liquids, Molten Salts, Polyelectrolytes*; Banneman, K. H., Ed.; Springer: Berlin, 1982; p 184.
- Rouse, P. E. *J. Chem. Phys.* **1953**, *21*, 1273.
- Zimm, B. J. *J. Chem. Phys.* **1956**, *24*, 269.
- (a) Stockmayer, W. H. *Pure Appl. Chem.* **1967**, *15*, 539. (b) Stockmayer, W. H.; Baur, M. E. *J. Am. Chem. Soc.* **1964**, *86*, 3485.
- Wijmenga, S. S.; van der Touw, F.; Mandel, M., to be published.
- Yamakawa, H. *Modern Theory of Polymer Solutions*; Harper and Row: New York, 1971.
- (a) Kirkwood, J. G.; Riseman, J. *J. Chem. Phys.* **1948**, *16*, 565. (b) Riseman, J.; Kirkwood, J. G. *J. Chem. Phys.* **1949**, *17*, 442.
- Benoit, H. *Ann. Phys.* **1951**, *6*, 561.
- (a) Weill, G.; des Cloizeaux, J. *J. Phys. (Paris)* **1979**, *40*, 99. (b) François, J.; Schwartz, T.; Weill, G. *Macromolecules* **1980**, *13*, 564.
- Odijk, T. *J. Polym. Sci., Polym. Phys. Ed.* **1977**, *15*, 477.
- Skolnick, J.; Fixman, M. *Macromolecules* **1977**, *10*, 944.
- Benoit, H.; Doty, P. *J. Phys. Chem.* **1953**, *57*, 958.
- Imai, N.; Ohinshi, T. *J. Chem. Phys.* **1959**, *30*, 1115.
- Manning, G. J. *J. Chem. Phys.* **1969**, *51*, 924.
- Odijk, T.; Mandel, M. *Physica* **1978**, *93*, 298.
- Odijk, T. *Polymer* **1978**, *19*, 989.
- Fixman, M.; Skolnick, J. *Macromolecules* **1978**, *11*, 863.
- Yamakawa, H.; Tanaka, G. *J. Chem. Phys.* **1967**, *47*, 3991.
- Odijk, T.; Houwaart, A. C. *J. Polym. Sci., Polym. Phys. Ed.* **1978**, *16*, 627.
- de Gennes, P. G. *J. Chem. Phys.* **1971**, *55*(2), 572.
- Edwards, S. F.; Grant, J. W. *J. Phys. A: Math., Nucl. Gen.* **1973**, *6*, 1169, 1186.
- Klein, J. *Macromolecules* **1978**, *11*, 852.